

On the transverse instability of the two-dimensional Benjamin–Ono solitons

Denis G. Gaidashev

Department of Mathematics, University of Toronto, Toronto, Ontario M5S 3G3, Canada

Sergey K. Zhdanov

Department of Plasma Physics, Moscow Engineering Physics Institute, Kashirskoe sh. 31, Moscow 115409, Russia

(Received 2 July 2003; accepted 23 February 2004; published online 29 April 2004)

The paper presents a stability analysis of plane solitons in hydrodynamic shear flows obeying a (2+1) analogue of the Benjamin–Ono equation. The analysis is carried out for the Fourier transformed linearized (2+1) Benjamin–Ono equation. The instability region and the short-wave instability threshold for plane solitons are found numerically. The numerical value of the perturbation wave number at this threshold turns out to be constant for various angles of propagation of the solitons with respect to the main shear flow. The maximum of the growth rate decreases with the increasing angle and becomes equal to zero for the perpendicular propagation. Finally, the dependency of the growth rate on the propagation angle in the long-wave limit is determined and the existence of a critical angle which separates two types of behavior of the growth rate is demonstrated. © 2004 American Institute of Physics. [DOI: 10.1063/1.1705649]

I. INTRODUCTION

Stability of nonlinear waves in various hydrodynamic models, in particular, stability of solitons, has been historically of much interest. Solitons were shown to be typical of many nonlinear evolution equations, extensive theoretical and experimental study of these objects undertaken by the present time has revealed the unique features of these waves. An interesting case of solitary waves in hydrodynamic flows is solitons propagating in a stationary shear flow. Stability of these waves is the focus of the present paper.

It has been shown^{1,2} that the propagation of one-dimensional internal waves in ideal deep stratified fluid is described by the well-known Benjamin–Ono equation

$$u_t + 6uu_x + \partial_x^2 \hat{H}[u] = 0, \quad (1)$$

where u is the horizontal velocity of the wave,

$$\hat{H}[u] = \frac{1}{\pi} P.V. \int_{-\infty}^{+\infty} \frac{u(x')}{x-x'} dx' \quad (2)$$

is the Hilbert transform of u and $P.V.$ stands for a principle value. The factor in front of the nonlinear term can be chosen to be an arbitrary constant by a simple rescaling. The most often used factors are 2 and 6.

It is not surprising that the Benjamin–Ono equation serves as a good model for the evolution of long, slightly nonlinear one-dimensional internal perturbations in media with other types of nonhomogeneity: The same equation has been shown to model propagation of disturbances in sheared boundary and surface flows of fluids.^{3,4} As it is the case with many other long-wave models, the Benjamin–Ono equation appears as the second-order approximation to a fully nonlinear system of the Euler equations expanded in a nonlinearity parameter, and should be expected to be relevant in a rather

wide range of hydrodynamic and magneto-hydrodynamic applications, not bound by a specific character of nonhomogeneity.

The Benjamin–Ono equation is known to have both periodic and soliton solutions. Its periodic solutions can be obtained by Hirota's direct method^{5,6} and can be represented as

$$u = \frac{1}{3} \frac{k_1 \cdot \tanh \phi_1}{\cos \xi_1} \frac{1}{\cosh \phi_1}, \quad \xi_1 = k_1(x - c_1 t) + \xi_1^{(0)}, \quad (3)$$

$$c_1 = k_1 \coth \phi_1,$$

where $\xi_1^{(0)}$ is a constant phase shift and parameters k_1 and ϕ_1 are positive constants, the first being the wave number, the second—the nonlinearity parameter. The case of the parameter $\phi_1 \rightarrow \infty$ leads to a harmonic wave of a small amplitude, while the case of $\phi_1 \rightarrow 0$ and $k_1 \rightarrow 0$ (keeping the ratio k_1/ϕ_1 bounded) gives a plane “algebraic” soliton [in this paper by “plane soliton” we shall mean the standard one-dimensional (1D) soliton, a “carpet roll” extending to infinities in the direction perpendicular to the direction of propagation] of the form

$$u = \frac{2}{3} \frac{S}{1 + (S\xi_1 - \Omega t)^2}, \quad S = \frac{k_1}{\phi_1}, \quad \Omega = S^2. \quad (4)$$

Bi-soliton solutions and multi-soliton solutions could be obtained by Hirota's method introducing more parameters k_i , ϕ_i , c_i , and variables ξ_i in a similar way.

A model for two-dimensional, slightly nonlinear internal waves in a hydrodynamic shear flow was first considered by Shrira.⁷ The model was derived without the assumption of the disparate scales along and across the flow [unlike, for example, in the Kadomtsev–Petviashvili (KP) equation—a

“two-dimensional” version of the Korteweg–de Vries (KdV) equation]. The derivation uses the multiple scale expansion of coordinates (x,y,z) , together with the velocity field $\mathbf{u}=(u,v,w)$ of the perturbation of the main flow $\mathbf{U}=(U(z),0,0)$ assumed to depend on the vertical coordinate z only, in the expansion parameter $\epsilon=kh$, where k is the wave number of the perturbation and h is the depth of the fluid. Expanding the Euler equations with the standard “solid” surface and bottom conditions up to the first order in ϵ , Shrira has obtained the well-known Rayleigh equation for the amplitude of the vertical velocity of the linear waves $W(z)\exp[i(\mathbf{k}\mathbf{x}-\omega t)]$ (here, z is the vertical coordinate, $\mathbf{x}=(x,y)$ are the horizontal coordinates):

$$(U(z)-c)(W''(z)-k^2W(z))-U''(z)W(z)=0. \tag{5}$$

Solutions (modes) of Eq. (5) are known to be stable in the limit $k\rightarrow 0$ for the flow profiles without points of inflection. It has been shown⁷ that in the long-wave approximation ($\epsilon\ll 1$) the linear analysis yields a localized mode

$$W(z)=(U-c)\exp[-k|z|], \tag{6}$$

with the dispersion relation

$$c=U(0)+k\frac{U^2(0)}{U'(0)}. \tag{7}$$

Next, if a small perturbation of the horizontal velocity of the main flow is written as $u(\mathbf{x},z,t)=\epsilon A(\mathbf{x},t)U'(\epsilon^{-1}z)$, the application of the multiple scale expansion up to terms of the second order in ϵ results in a nonlinear integro-differential equation for the amplitude $A(\mathbf{x},t)$:

$$A_t+\nu A_x+sAA_x-r\hat{G}[A_x]=0, \tag{8}$$

where $\hat{G}[A(\mathbf{x},t)]=\int\int k'A(\mathbf{x}',t)\exp[i\mathbf{k}'(\mathbf{x}-\mathbf{x}')] \partial\mathbf{x}'\partial\mathbf{k}'$ and $\nu=U(0)$, $s=U'(0)$, $r=U^2(0)/U'(0)$. Here, we have used the notation $\mathbf{x}=(x,y)$, $\mathbf{k}=(k_x,k_y)$, and $k=(k_x^2+k_y^2)^{1/2}$. We shall call Eq. (8) the Shrira equation after its author. It should be noted that this equation is a two-dimensional analogue of the Benjamin–Ono equation and coincides with the latter in the reduction $A(\mathbf{x},t)=A(x,t)$.

A theoretical analysis of the transverse instability of the plane Benjamin–Ono solitons in the two-dimensional case⁸ shows that such solitons should possess a self-focusing instability which results in a “two-dimensionalization” and a collapse at later stages; an earlier numerical simulation⁹ also indicates the possibility of existence of essentially two-dimensional formations within the framework of the model.

The subject of this paper, the transverse instability of oblique solitons, has been studied¹⁰ analytically for very long transverse perturbations of the amplitude and numerically in the general case. It is worth noting this numerical analysis¹⁰ gives an atypical dependence of the instability growth rate on the perturbation wave number. For large inclination angles of solitons this dependence becomes oscillating, eventually, for angles close to $\pi/2$ there appear many regions of instability with the growth rate intermittently increasing to a positive maximum and dropping back to zero as the perturbation wave number increases.

Finally, we would like to remark that (8) can serve as a model equation in some magneto-hydrodynamic systems in plasma physics, in particular it is easy to show that the Shrira equation describes the amplitude of the perturbation of the horizontal velocity component of a sheared flow of electrons. Solitons of this equation have not been discussed in plasma applications, but taking into consideration the fact that non-uniform flows are typical for plasmas, one could expect that algebraic solitons might appear in such systems.

II. TRANSVERSE INSTABILITY OF SOLITONS OF THE SHRIRA EQUATION

A. Transverse perturbations of the Shrira equation

The substitution

$$A=-\frac{6r}{s}u, \quad \tilde{t}=-\frac{t}{r}, \quad c=-\frac{\nu}{r} \tag{9}$$

transforms Eq. (8) into one of the standard Benjamin–Ono forms (after dropping tildes over the time variable):

$$u_t+cu_x+6uu_x+\hat{G}[u_x]=0. \tag{10}$$

The above equation, or its version in the frame fixed on the main flow

$$u_t+6uu_x+\hat{G}[u_x]=0, \tag{11}$$

clearly has plane solitons

$$u_0=\frac{2}{3}\frac{S}{1+(Sx-\Omega t)^2}, \quad \Omega=S^2, \tag{12}$$

as one of its solutions. In fact, as we mentioned before, on a restricted class of functions, independent of y , the Shrira equation reduces to the Benjamin–Ono equation. In what follows we want to consider a more general class of solutions of (8)—solitons propagating at an arbitrary angle α to the main flow

$$u_0=\frac{2}{3}\frac{S}{1+(\mathbf{S}\cdot\mathbf{x}-\Omega t)^2}, \tag{13}$$

where $\mathbf{S}=(S\cos\alpha,S\sin\alpha)$ and $\Omega=S^2\cos\alpha$.

It is a well-known fact that the Benjamin–Ono solitons (as well as Shrira solitons propagating at a certain angle) are stable against the longitudinal perturbations. However, the situation changes dramatically when one considers the transverse perturbations. In this case, as we are about to show, the solitons are unstable.

First, we shall find an equation which allows us to analyze the instability. To this end we consider the perturbation $\tilde{u}(\xi,\eta,t)=\theta(\xi)\exp[i(\omega t+k_\eta\eta)]$, with $\theta(\xi)$ being a function with a compact support, in the coordinate frame, oriented with the soliton

$$\begin{bmatrix} \xi \\ \eta \end{bmatrix} = \begin{bmatrix} \cos\alpha & \sin\alpha \\ -\sin\alpha & \cos\alpha \end{bmatrix} \cdot \begin{bmatrix} x-ct \\ y \end{bmatrix}, \tag{14}$$

where c is the (rescaled) velocity of the main flow (at a fixed depth), and proceed to linearize (10) obtaining an equation for $\theta(\xi)$:

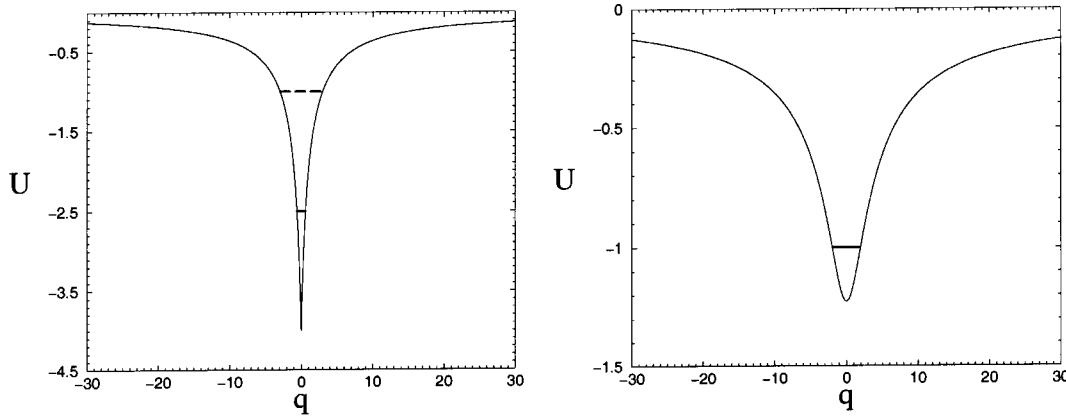


FIG. 1. (a) Energy levels at the long-wave instability threshold: The ground state (solid line) and the first “excited” state (dashed line). (b) Energy levels at the short-wave instability threshold: The ground state (solid line).

$$i\omega\theta(\xi) = \partial_x \left[c\theta(\xi) - 6u_0\theta(\xi) - \frac{1}{2\pi}(k_\eta^2 - \partial_\xi^2) \right. \\ \left. \times \int \frac{\exp[ik'_\xi(\xi - \xi')]\theta(\xi')}{[(k'_\xi)^2 + k_\eta^2]^{1/2}} \partial k'_\xi \partial \xi' \right], \quad (15)$$

where $\partial_x = \cos \alpha \cdot \partial_\xi - \sin \alpha \cdot ik_\eta$.

Equation (15) has been previously obtained in Ref. 10. Using an asymptotic representation of the integrand in (15) the problem was restated as an eigenvalue problem for small wave numbers and solved via Hirota’s method. Thus obtained growth rate for the quasi-periodic nonlinear wave is given by $\gamma^2 = c^2 k_y^2 - k^2[(K - k_x)^2 + k_y^2]$ where K is expressed through the nonlinearity parameter ϕ , $K\sigma = \tan \phi$. This expression for the growth rate shows that the instability region increases with the increasing nonlinearity of the wave (decreasing $K\sigma$).

We will, however, take a different course of action and cast Eq. (15) in a form especially convenient for numerical analysis. To that end, we perform the transformation $\phi(q) = \int \tilde{\theta}(q') \exp[-\sigma|q - q'|] \partial q'$, where $\tilde{\theta}(q)$ is the Fourier transform of $\theta(\xi)$. The new equation reads

$$\phi_{qq} + [-\sigma^2 - U]\phi = 0, \quad (16)$$

where

$$U = \frac{4\sigma^2}{1 + \sigma[q^2 + k_\eta^2]^{1/2} - \frac{\Omega}{q - k_\eta \tan \alpha}}, \quad (17) \\ \Omega = \frac{\sigma\omega}{\cos \alpha}, \quad \sigma = \frac{1}{c}.$$

Equation (16) presents a Sturm–Liouville problem with the boundary conditions $\phi(\pm\infty) = 0$. The potential U is complex in general (if the spectral parameter Ω is complex).

Some further analysis shows that there is an interesting connection between the structure of the levels in the potential U and the instability of solitons. This potential is real on the long-wave and short-wave instability thresholds, when the imaginary part of ω becomes equal to zero, and it is complex

in-between. A good illustration of the dynamics of the levels in such potential could be presented for zero angles of propagation. In this case the potential consists of an even real part and an odd imaginary (see Sec. II C for more details). This means that the real part of an eigenfunction of (16) is strictly even and the imaginary part is strictly odd, or vice versa. Thus, since the perturbation wave number is equal to 0 at the long-wave threshold, the odd one-node eigenfunction of (16) is either strictly real or strictly imaginary and the energy $E = -\sigma^2$ corresponds to the first energy level in the potential. Further, as k increases the wave function becomes complex, but turns even and either imaginary or real at the short-wave threshold where the potential is more shallow ($E = -\sigma^2$ is kept fixed) than at the long-wave threshold. This is the wave function of the ground state [see Figs. 1(a) and 1(b)]. At larger k the potential U has no level with $E = -\sigma^2$, thus rendering the instability impossible.

B. Transverse perturbations of Shrira solitons in long-wave approximation and the critical angle

In this section we apply expansion in a small parameter to obtain the growth rate of the oblique solitons in the long-wave limit. For this, we first expand the potential in Eq. (16) for small k_η (to simplify the notation we put $\sigma = 1$)

$$U = \frac{-4}{1 + |q|} \left(1 + \frac{-\frac{k_\eta^2}{2|q|} + \frac{\Omega}{q} + \frac{\Omega k_\eta \tan \alpha}{q^2}}{1 + |q|} + \frac{\frac{\Omega^2}{q^2}}{(1 + |q|)^2} \right). \quad (18)$$

Now, Eq. (16) is reduced to the form

$$\hat{L}[\phi] \equiv \left(\partial_q^2 - 1 + \frac{4}{1 + |q|} \right) \phi \\ = \left(\frac{2k_\eta^2}{|q|} - \frac{4\Omega}{q} - \frac{4\Omega k_\eta \tan \alpha}{q^2} - \frac{4\Omega^2}{q^2} \right) \phi. \quad (19)$$

TABLE I. Values of ω and γ for initial data $\omega=0.5$ and $\gamma=1.0$.

| Number of points | $\omega - n(n+1)$ | γ | Number of iterations |
|------------------|-------------------|-----------|----------------------|
| 100 | -8.07E-04 | -8.90E-07 | 11 |
| 500 | -3.36E-05 | -7.50E-07 | 10 |
| 1000 | -9.37E-06 | -7.51E-07 | 12 |
| 2000 | -3.31E-06 | -7.46E-07 | 11 |
| 3000 | -2.20E-06 | -7.51E-07 | 15 |
| 4000 | -1.81E-06 | -7.54E-07 | 16 |

Introduce a dimensionless book-keeping parameter ϵ and write $k_\eta = \epsilon \kappa_\eta$ (one thinks of κ_η as a quantity of order one). Now, one can attempt to find the complex frequency and the eigenfunction as a series in ϵ :

$$\Omega = \Omega_1 \epsilon + \Omega_2 \epsilon^2 \dots, \tag{20}$$

$$\phi = \phi_0 + \phi_1 \epsilon + \phi_2 \epsilon^2 \dots. \tag{21}$$

This will allow us to isolate consecutive orders in Eq. (19). Equating terms of the same order we get

$$\hat{L}[\phi_0] = 0, \tag{22}$$

$$\hat{L}[\phi_1] = -\frac{4\Omega_1 \phi_0}{q(1+|q|)^2}, \tag{23}$$

$$\hat{L}[\phi_2] = \frac{2\kappa_\eta^2 \phi_0}{|q|(1+|q|)^2} - \frac{4\Omega_1 \phi_1}{q(1+|q|)^2} - \frac{4\Omega_2 \phi_0}{q(1+|q|)^2} - \frac{4\Omega_1 \kappa_\eta \tan \alpha \phi_0}{q^2(1+|q|)^2} - \frac{4\Omega_1^2 \phi_0}{q^2(1+|q|)^3}. \tag{24}$$

The first and the second of these equations can be easily solved to get

$$\phi_0 = q(1+|q|)\exp[-|q|], \tag{25}$$

$$\phi_1 = -\Omega_1(\exp[-|q|] + 2q(1+q)\eta(q)\exp[-q]), \tag{26}$$

where $\eta(q)$ is the step function.

We notice that because of Eq. (22) and the self-adjoint property of \hat{L} the following condition should necessarily hold for all orders of ϕ :

$$\int \phi_0 \hat{L}[\phi_i] \partial q = 0. \tag{27}$$

Now, this condition for ϕ_1 is satisfied, as can be easily checked. The same condition in the next order gives a non-trivial equation

$$\int \phi_0 \hat{L}[\phi_2] \partial q = 0 = \frac{\kappa_\eta^2}{2} + \Omega_1^2 - 2\kappa_\eta \Omega_1 \tan \alpha, \tag{28}$$

from which we obtain the dispersion relation in the long-wave limit (we drop the ordering subscripts and reinstate our notation for the wave number)

$$\Omega = k_\eta \sin \alpha \pm i \cos \alpha \left(\frac{k_\eta^2}{2} - k_\eta^2 \tan^2 \alpha \right)^{1/2}. \tag{29}$$

Of the special importance is the fact that this dispersion brings about the existence of a critical angle. Two different

TABLE II. Values of ω and γ for initial data $\omega=31.0$ and $\gamma=2.0$.

| Number of points | $\omega - n(n+1)$ | γ | Number of iterations |
|------------------|-------------------|-----------|----------------------|
| 100 | 2.76 | -7.63E-07 | 7 |
| 500 | -1.21E-02 | 4.86E-07 | 7 |
| 1000 | -3.05E-03 | 4.72E-07 | 8 |
| 2000 | -7.77E-04 | 4.39E-07 | 7 |
| 3000 | -3.56E-04 | 4.32E-07 | 7 |
| 4000 | -2.08E-04 | 4.30E-07 | 8 |

scenarios for the growth rate are separated by the angle $\alpha_c = \arctan(1/\sqrt{2})$. The growth rate itself is given by

$$\gamma = \cos \alpha \cdot \frac{k_\eta}{\sqrt{2}} (1 - 2 \tan^2 \alpha)^{1/2}, \tag{30}$$

and for $\alpha > \alpha_{cr}$ it follows the tendency $\gamma/k_\eta \rightarrow 0$ as $k_\eta \rightarrow 0$, while for $\alpha < \alpha_{cr}$, $\gamma/k_\eta \rightarrow \text{const}$.

It is worth noting that the case of $\alpha=0$ yields $\omega=0$ and $\gamma=k_\eta/\sqrt{2}$ —a result which has been previously obtained in the literature.⁸

The above analysis shows that in the long-wave approximation the decay rate grows linearly with the perturbation wave number.

C. Numerical analysis of the instability

The main result of this paper is the dependence of the instability growth rate and the real frequency on the perturbation wave number for several angles of propagation. To this end we proceed to analyze Eq. (16) numerically.

To limit the range of the independent variable in (16) we used the following substitution:

$$x = \frac{2}{\pi} \arctan(q). \tag{31}$$

Taking into account the fact that in the most general case of an arbitrary angle of propagation the potential in (16) is complex, substitution (31) transforms the Sturm–Liouville equation (16) into an equation for a complex eigenfunction $\phi(x)$

$$\frac{4 \cos^4\left(\frac{\pi x}{2}\right)}{\pi^2} \phi'' - \frac{4 \cos^4\left(\frac{\pi x}{2}\right) \tan\left(\frac{\pi x}{2}\right)}{\pi} \phi' + (-\sigma^2 - U(x)) \phi = 0, \tag{32}$$

where

$$U(x) = \frac{-4\sigma^2}{1 + \sigma \left[\tan\left(\frac{\pi x}{2}\right)^2 + k_\eta^2 \right]^{1/2}} - \frac{\Omega}{\tan\left(\frac{\pi x}{2}\right) - k_\eta \tan \alpha}. \tag{33}$$

We discretize this equation using the standard two-point approximation for the first derivative and three-point approximation for the second derivative, obtaining a linear problem for the vector of point-values of the complex eigen-

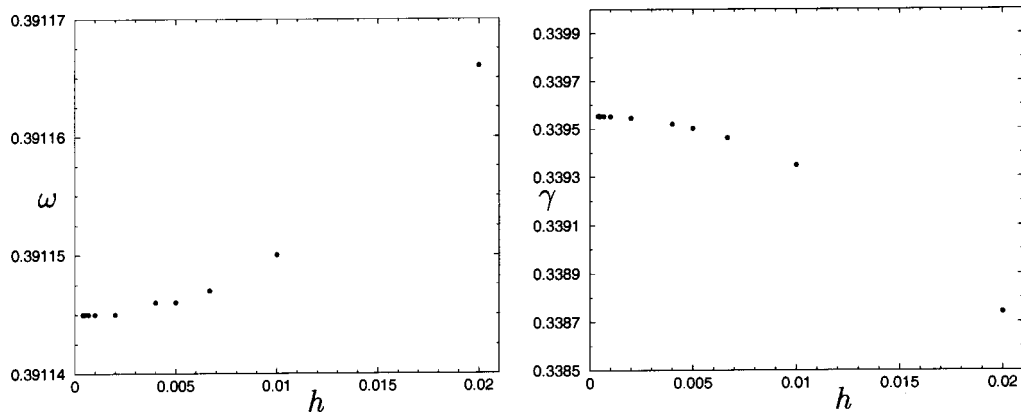


FIG. 2. (a) ω as a function of the discretization step h for $\alpha=\pi/6, k=1.0$. (b) γ as a function of the discretization step h for $\alpha=\pi/6, k=1.0$.

function, \mathbf{e} . This problem, of the form $\mathbf{A}\mathbf{e}=0$, where \mathbf{A} is some matrix, together with the zero boundary conditions at $x=1$ and $x=-1$, has a nontrivial solution if the complex determinant $\det(\mathbf{A})(\omega, \gamma, k)=0$, where $\omega=\text{Re}[\Omega]$ and $\gamma=\text{Im}[\Omega]$. We solve this equation for each value of k using the standard two-dimensional (2D) globally convergent Newton method with line search and backtracking.¹¹

To test the viability of the method, first we try it on a Sturm–Liouville problem with the soliton-like complex potential

$$U(x) = -\omega \operatorname{sech}^2\left(\tan\left(\frac{\pi x}{2}\right)\right) - i\gamma \operatorname{sech}^2\left(\tan\left(\frac{\pi x}{2}\right)\right). \tag{34}$$

The real part of this potential is the famous attracting KdV-soliton appearing in the direct problem for the KdV equation. It is a well-known fact that the Sturm–Liouville problem with such complex potential and zero-boundary conditions possesses an eigenvalue $\lambda=-1$ for $\omega=n(n+1)$, $\gamma=0$. These values of ω and λ correspond to the $(n-1)$ st energy level in the soliton well.¹²

We ran our root-finding procedure for several discretizations of the interval $(-1,1)$. Here we include the results of convergence of ω and γ to the required values for two initial approximations: $\omega=0.5, \gamma=1.0$ and $\omega=31.0, \gamma=2.0$. The first set of data is expected to converge to $\omega=2.0, \gamma=0.0$ ($n=1$) and the second to $\omega=30.0, \gamma=0.0$ ($n=5$).

The values of ω and γ (rounded up to 3 significant figures) and the number of iterations in the Newton root-finding are summarized in Tables I and II.

For this test the convergence criterion on the function value in the Newton procedure was kept at $1.0E-14$, the step convergence criterion at $1.0E-16$ and criterion of convergence on a spurious minimum at $1.0E-15$. For all discretizations the Newton root-finding was terminated by step convergence.

As a further demonstration of the method we include the convergence results of our algorithm for various discretizations of the Sturm–Liouville problem with the potential (33). The results for the angle $\alpha=\pi/6$ and the perturbation wave number $k=1.0$ are given in Figs. 2(a) and 2(b) and Table III. The first column is the value of the step used in the discretization of the equation, the second and the fourth columns are the obtained values of ω and γ , the third and the fifth columns show the difference of ω and γ values for two consecutive discretizations. All differences are rounded up to three significant figures. The convergence is obviously superlinear and probably quadratic as it should be expected for a second-order scheme.

Thus tested algorithm was used to compute the dispersion curves of the perturbed Shrira equation. The obtained dependencies are pictured in Figs. 3(a) and 3(b).

These curves do show the expected behavior: Solitons propagating along the flow are the most unstable, instability decreases with the increasing angle of propagation eventually disappearing for perpendicular solitons.

It should be noted that the obtained instability growth rate dependence on the transverse perturbation wave number is quite similar to those typical of many well-known classical

TABLE III. Convergence of the real frequency and the growth rate for several discretizations of (29).

| h_i | ω_i | $\omega_i - \omega_{i-1}$ | γ_i | $\gamma_i - \gamma_{i-1}$ |
|------------|---------------|---------------------------|---------------|---------------------------|
| 2.0E-02 | 0.391 165 562 | | 0.338 741 227 | |
| 4.0E-03 | 0.391 145 659 | -1.99E-5 | 0.339 520 253 | 7.79E-4 |
| 2.0E-03 | 0.391 144 974 | -6.85E-7 | 0.339 544 804 | 2.45E-5 |
| 1.0E-03 | 0.391 144 802 | -1.72E-7 | 0.339 550 943 | 6.12E-6 |
| 6.6(6)E-04 | 0.391 144 769 | -3.3E-8 | 0.339 552 079 | 1.14E-6 |
| 5.0E-04 | 0.391 144 758 | -1.1E-8 | 0.339 552 477 | 3.98E-7 |
| 4.0E-04 | 0.391 144 753 | -5.0E-9 | 0.339 552 661 | 1.84E-7 |
| 3.51E-04 | 0.391 144 750 | -3.0E-9 | 0.339 552 737 | 7.6E-8 |

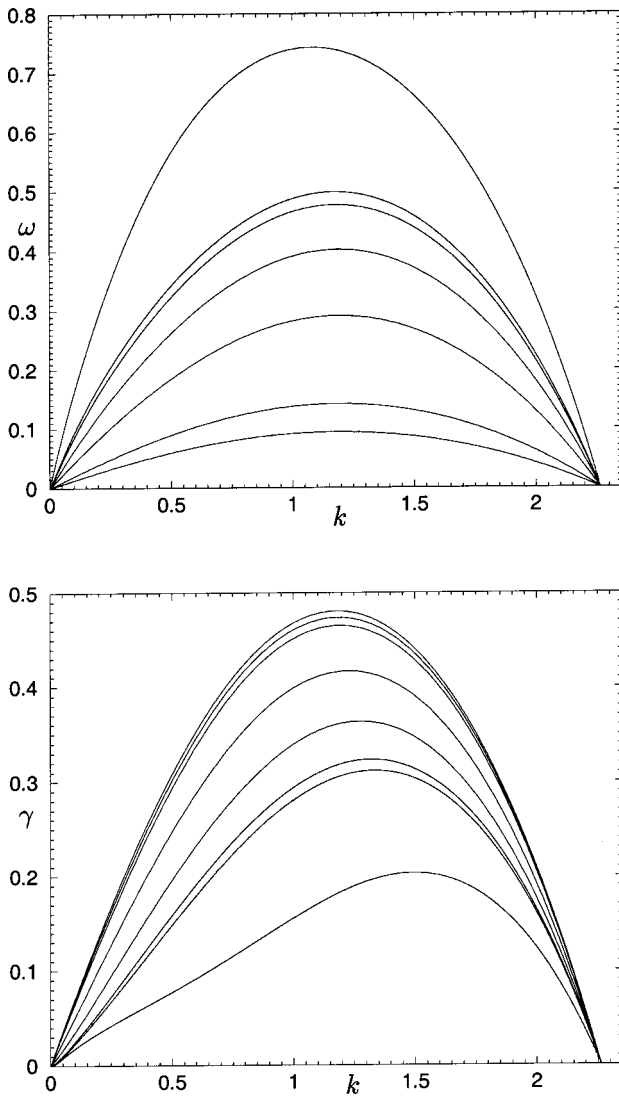


FIG. 3. (a) Dependence of the real frequency ω on the wave number k for several angles of propagation (in radians, top to bottom): $\pi/4, 0.62, 0.60, \pi/6, \pi/8, \pi/16, \pi/24$. (Remark: The frequency curve for angle 0 coincides with the horizontal axis.) (b) Dependence of the growth rate γ on the wave number k for several angles of propagation (in radians, top to bottom): $0, \pi/24, \pi/6, \pi/8, \pi/6, 0.60, 0.62, \pi/4$.

nonlinear wave models such as KdV, KP, and NSE. If a soliton described by this model is unstable against the transverse perturbation then, at the long-wave end of the instability range, growth rate increases with increasing wave number, further, for shorter waves the dynamics is stabilized when the wavelength is of the order of characteristic length defined by dispersion.

In contrast to the earlier obtained results,¹⁰ there are no multiple zones of instability within the instability range, rather, there exists a single universal zone of instability, and the short wave threshold turns out constant for all angles of soliton inclination.

In an attempt to justify our predictions of Sec. II B for the long-wave growth rate behavior we used our numerical scheme for small k and for two angles, above and below the predicted critical angle. Results, shown in Fig. 4, do confirm the existence of a critical angle, separating two types of be-

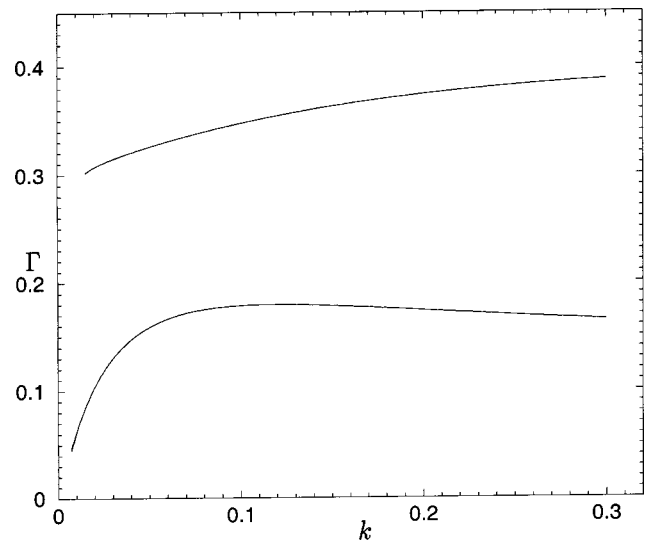


FIG. 4. Dependence of the growth rate divided by the wave number, Γ , on the wave number k for two angles of propagation, above and below the critical: $\pi/6$ (upper curve) and $\pi/4$ (lower curve).

havior. A remark, however, is in order: We were not able to implement the algorithm all the way to $k=0$. For very small k and Ω the potential becomes very irregular and our numerical scheme produces (spurious) oscillations in the dispersion curves. Despite of this, tendencies of γ/k for angles above and below critical are obviously in accord with the predictions of Sec. II B.

D. Stability of solitons propagating perpendicular to the main flow

The “perpendicular” solitons, i.e., solitons moving at the angle $\pi/2$ to the main flow have been shown to be stable.¹⁰ We would like to briefly illustrate how this stability comes about in our approach. Below, we will restrict our exposition to the case of long-wave perturbations when Eq. (16) could be rewritten as

$$\phi_{qq} + [-1 - U]\phi = 0, \tag{35}$$

$$U = -\frac{4}{1 + |q| - \nu}, \quad \nu = \left[\frac{\Omega \cos \alpha}{k_\eta} \right]_{k_\eta \rightarrow 0}, \tag{36}$$

where we have put for simplicity $\sigma=1$ which is equivalent to the change of variables $\sigma q \rightarrow q$. Matching the relatively self-suggesting solutions of (35) and their derivatives for negative and positive values of q we were able find two even solutions:

$$\phi_0 = (\nu_0 + |q|) \cdot (1 + \nu_0 + |q|) \exp[-|q|], \quad \nu_0 = \frac{1 + \sqrt{5}}{2}, \tag{37}$$

$$\phi_2 = (\nu_2 + |q|) \cdot (1 + \nu_2 + |q|) \exp[-|q|], \quad \nu_2 = \frac{1 - \sqrt{5}}{2}, \tag{38}$$

and two odd ones:

$$\phi_1 = q \cdot (1 + |q|) \exp[-|q|], \quad \nu_1 = 0, \tag{39}$$

$$\phi_3 = q \cdot (1 - |q|) \exp[-|q|], \quad \nu_3 = -1. \quad (40)$$

It can be seen that the value ν_0 of the spectral parameter ν corresponds to the eigenfunction without zeros, that is an eigenfunction of the ground state of the potential U . The value ν_1 corresponds to the one-node function of the first state, the value ν_2 corresponds to the eigenfunction of the second state with two nodes and the value ν_3 —to the eigenfunction of the third level with three nodes. The depth of the potential is different for these parameter values, while the energy of the corresponding state is constant and equal to -1 . Of the special importance is the fact that all parameter values are real. This means that for the “perpendicular” solitons

$$[k_\eta \nu_i]_{k_\eta \rightarrow 0} = [\Omega \cos \alpha]_{\alpha \rightarrow \pi/2} = \omega, \quad (41)$$

the perturbation frequency is real and the four perturbation modes (37)–(40) are stable. This is in line with (30) since the instability growth rate should go to zero faster than k_η for angles larger than the critical, and $\pi/2$ is certainly larger than α_{cr} .

III. CONCLUSION

We have considered stable and unstable dynamics of oblique Benjamin–Ono solitons in shear hydrodynamic flows. Several aforementioned results are worth emphasizing.

First, the value of the short-wave threshold of the transverse perturbation of the solitons turned out to be constant and independent of the angle of propagation of the soliton with respect to the main shear flow. We determined this value numerically to be $k_{th}/c = 2.2625 \pm 0.0005$ where c is the velocity of the main flow.

Second, using numerical methods we found the dependence of the instability growth rate and the real frequency on the perturbation wave number for several angles of propagation. Numerical calculations show that the maximum of the

growth rate decreases with the growth of the propagation angle and becomes equal zero for $\pi/2$. For a fixed angle both the growth rate and the real frequency monotonously grow with the perturbation wave number to a certain maximum, then monotonously decrease and become equal zero at the short-wave threshold.

Lastly, analytic considerations allowed us to predict the character of the growth rate dependency on the propagation angle for long waves. We have shown that there exists a critical angle of propagation in the long-wave limit which serves as a border between two different behaviors of the growth rate: $\gamma/k_\eta \rightarrow 0$ for $\alpha > \alpha_{cr}$ and $\gamma/k_\eta \rightarrow \text{const}$ for $\alpha < \alpha_{cr}$.

¹T. B. Benjamin, “Internal waves of permanent form in fluids of great depth,” *J. Fluid Mech.* **29**, 559 (1967).

²H. Ono, “Algebraic solitary waves in stratified fluids,” *J. Phys. Soc. Jpn.* **39**, 1082 (1975).

³V. I. Zhuk and O. S. Ryshov, “On locally inviscid disturbances in a boundary layer with self-induced pressure,” *Dokl. Akad. Nauk SSSR* **263**, 56 (1982).

⁴N. N. Romanova, “Long nonlinear waves on layers having large wind velocity gradients,” *Izv., Acad. Sci., USSR, Atmos. Oceanic Phys.* **20**, 469 (1984).

⁵R. Hirota, “Direct method of finding exact solutions of nonlinear evolution equations,” *Lect. Notes Math.* **515**, 40 (1976).

⁶J. Satsuma and Y. Ishimori, “Periodic wave and rational soliton solutions of the Benjamin–Ono equation,” *J. Phys. Soc. Jpn.* **46**, 681 (1979).

⁷V. I. Shrira, “On surface waves in the upper quasi-uniform ocean layer,” *Dokl. Akad. Nauk SSSR* **308**, 732 (1989).

⁸A. N. Dyachenko and E. A. Kuznetsov, “Instability and self-focusing of solitons in the boundary layer,” *JETP Lett.* **59**, 108 (1994).

⁹L. A. Abramyan, Yu. A. Stepanyants, and V. I. Shrira, “Multidimensional solitons in shear flows of the boundary-layer type,” *Sov. Phys. Dokl.* **37**, 575 (1992).

¹⁰D. E. Pelinovsky and Yu. A. Stepanyants, “Self-focusing instability of solitons in shear flows,” *JETP* **78**, 883 (1994).

¹¹W. H. Press, B. P. Flannery, S. A. Teukolsky, and W. T. Vetterling, *Numerical Recipes in Fortran. The Art of Scientific Computing* (Cambridge University Press, Cambridge, 1992).

¹²G. L. Lamb, *Elements of Soliton Theory* (Wiley, New York, 1980).